2016 International Symposium on Nonlinear Theory and Its Applications,
NOLTA2016, Yugawara, Japan, November 27th-30th, 2016

Modeling of Effective Heat Diffusion in a Building Atrium via Koopman Mode Decomposition

Yohei Kono[†1], Yoshihiko Susuki[†2], Mitsunori Hayashida[‡3], and Takashi Hikihara[†]

†Department of Electrical Engineering, Kyoto University
Nishikyo, Kyoto 615-8510, Japan
‡Environmental Busuiness Headquaters, OMRON Corporation
Shiokoji-Horikawa, Shimogyo, Kyoto 600-8530, Japan
Email: y-kono@dove.kuee.kyoto-u.ac.jp

Abstract—We develop a method for modeling of heat transfer dynamics in a building atrium based on observational data on temperature. This paper introduces a two-dimensional heat diffusion equation with an effective diffusion coefficient in order to represent the heat transfer mainly due to the air movement inside an atrium, where the air slowly moves on a length-scale smaller than the distance between rooms. Then we propose a method for identifying the coefficient based on a spatio-temporal oscillatory pattern extracted from the data via Koopman mode decomposition. The calculated coefficient is verified with the characteristic numbers of the air flow in the atrium and its architectural geometry.

1. Introduction

In-building energy dynamics appear on a wide range of scales in both space and time. In the stage of architectural design, lumped-parameter models are used in order to predict coarse-scale thermal dynamics: see e.g. [1]—ranges of more than lengths between rooms. The models have focused on the heat transfer via walls, ceilings, or floors with large time-constant about 100 hours. On the other hand, the heat transfer in a building atrium is on smaller time-scale [2], and thus a short-term change of in-room temperature can propagate between rooms. Therefore, mathematical modeling of the heat transfer in an atrium is required for its evaluation and control.

In this paper, we adress the phenomenon of heat transfer mainly due to the air movement inside a practically-used atrium, where the air slowly moves on a length-scale smaller than the distance between rooms. The heat transfer is modeled as a two-dimensional heat diffusion equation with an effective diffusion coefficient. Then we propose a method for identifying the coefficient based on a spatio-temporal oscillatory pattern extracted from measurement data via Koopman mode decomposition [3, 4]. The calculated coefficient is verified with the characteristic numbers of fluid flow in the atrium and its architectural geometry.

2. Modeling target in commercial building

This paper focuses on a practically-used atrium in order to delinate the modeling idea. This atrium is located in the main building of OMRON Healthcare Co., Ltd. in Kyoto, Japan. This section provides basic information on the atrium as the modeling object: spatial arrangements and operational conditions of HVAC units, and the measurement of temperature.

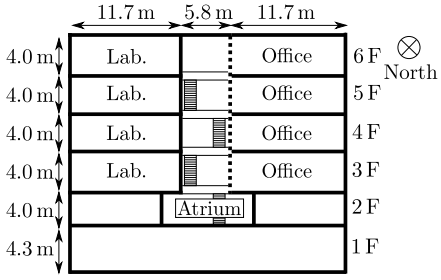

Figure 1: Cross section of the target building.

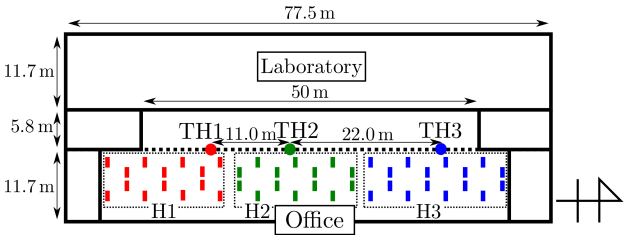

Figure 2: Outline of 3rd to 6th floors of the target building. The circles stand for temperature sensors and the rectangles for outlet ducts.

Figures 1 and 2 show the cross section of the target building and the outline of a floor. The building consists of six floors, where the eastern sides of the 3rd to 6th floors are provided as office rooms and the western sides as laboratories. The atrium is located in the center of the building and connected with the office rooms.

Next, we review spatial arrangements and operational conditions of HVAC units. Three HVAC units are placed in the office room for conditioning globally in space. In the below, these units are called H1, H2, and H3. Their outlet ducts are on the ceiling and denoted by the rectangular symbols. The red, green, and blue symbols represent the ducts of H1, H2, and H3, respectively. The HVAC units run on a programed schedule.

Finally, we review the measurement system of temperature in the target building. All the temperature data were

[1]Present affiliation: Research & Development Group, Hitachi, Ltd.
[2]Present affiliation: Department of Electrical and Information Systems, Osaka Prefecture University
[3]Present affiliation: Technology Creation Center, OMRON SOCIAL SOLUTIONS Co.,Ltd.

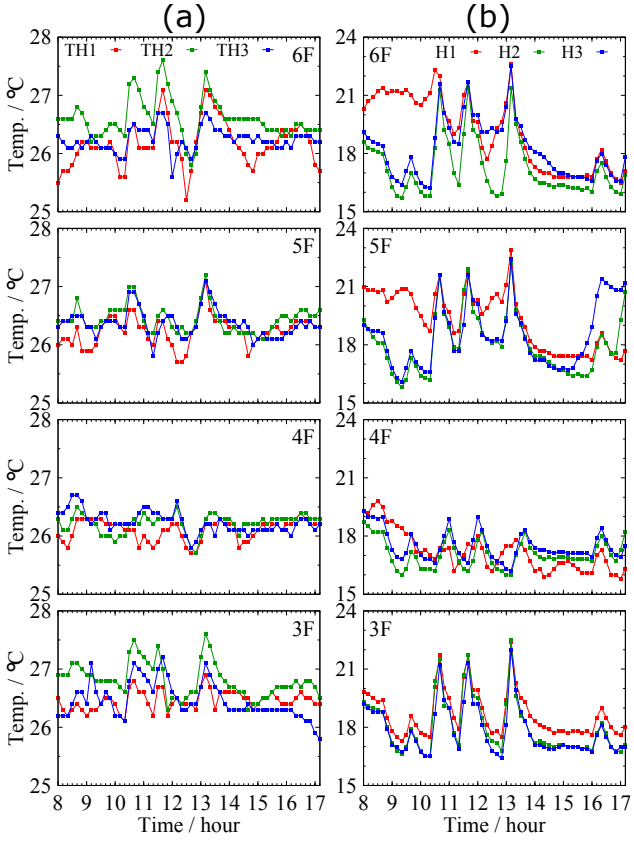

Figure 3: Data sampled on July 31, 2014 (Thu.): (a) atrium temperature and (b) outlet temperature.

sampled by 0.1 °C every 10 minutes. Atrium temperature is sampled by three sensors on each floor. These sensors are placed at the height 1.5 m above the floor. They are denoted in Fig. 2 with circles and called TH1, TH2, and TH3. Also, outlet temperature of H1, H2, and H3 was sampled. Figure 3 shows the atrium temperature and outlet temperarue sampled on July 31, 2014 (Thu.). Both the temperatures oscillate on the time-scale of several hours.

3. Koopman mode decomposition of measured data

This section applies the Koopman Mode Decomposition (KMD) to the measured data on temperature shown in Fig. 3.

3.1. Outline

KMD is a method for extracting spatio-temporal modes oscillating with single frequencies directly from data [3, 4]. In this paper, we use the Arnoldi-type algorithm [4] to decompose snapshots $\boldsymbol{X}[n] \in \mathbb{R}^M$ $(n = 0, \ldots, N-1)$ with constant time-step Δt into the following series:

$$\boldsymbol{X}[n] = \sum_{m=1}^{N-1} \tilde{\lambda}_m^n \tilde{\boldsymbol{V}}_m \quad (n = 0, \ldots, N-2), \tag{1}$$

where $\tilde{\lambda}_m \in \mathbb{C}$ is Koopman Eigenvalue (KE) and $\tilde{\boldsymbol{V}}_m \in \mathbb{C}^M$ is Koopman Mode (KM).

Table 1: Koopman mode decomposition of the data measured on July 31, 2014 (Thu.) shown in Fig. 3.

$\{m, m+1\}$	$\lvert\lambda_m\rvert$	T_m / h	$\lVert\boldsymbol{V}_m^{\mathrm{A}}\rVert$	$\lVert\boldsymbol{V}_m^{\mathrm{H}}\rVert$
$\{1, 2\}$	1.050	2.37	7.83×10^{-2}	0.286
$\{3, 4\}$	1.035	4.74	5.62×10^{-2}	0.695
$\{\mathbf{5}, \mathbf{6}\}$	1.035	**3.35**	**0.119**	**0.540**
$\{7, 8\}$	1.033	1.16	5.52×10^{-2}	0.339
$\{9, 10\}$	1.033	1.86	9.31×10^{-2}	0.262
$\{11, 12\}$	1.026	0.547	2.34×10^{-2}	0.116

Here, we formulate spatio-temporal oscillatory pattern of KM as a wave propagation. Let be m-th KE defined as $\tilde{\lambda}_m = |\tilde{\lambda}_m| \exp(\mathrm{i}\omega_m \Delta t)$, where i is the imaginary unit and ω_m is the angular frequency. Then the oscillatory pattern of m-th KM is represented as follows:

$$\tilde{\lambda}_m^n \tilde{\boldsymbol{V}}_m = |\tilde{\lambda}_m|^n \begin{bmatrix} A_{m,1} \exp\{\mathrm{i}(\omega_m n \Delta t + \theta_{m,1})\} \\ \vdots \\ A_{m,M} \exp\{\mathrm{i}(\omega_m n \Delta t + \theta_{m,M})\} \end{bmatrix}, \tag{2}$$

where $A_{m,p}$ and $\theta_{m,p}$ stand for modulus (amplitude) and angle (phase) of p-th component of KM $\tilde{\boldsymbol{V}}_m$, respectively. Now we represent the observation positions of data by using $\boldsymbol{r}_1, \ldots, \boldsymbol{r}_M \in \mathbb{R}^{N_{\mathrm{d}}}$ $(N_{\mathrm{d}} \in \{1, 2, 3\})$ and transposition of vector by the superscript T. When the matrix $[\boldsymbol{r}_1^{\mathsf{T}}, \ldots, \boldsymbol{r}_M^{\mathsf{T}}]$ is of full rank, it is possible to uniquely determine $\boldsymbol{k}_m \in \mathbb{R}^{N_{\mathrm{d}}}$ satisfying $\boldsymbol{r}_p^{\mathsf{T}} \boldsymbol{k}_m = -\theta_{m,p}$ for $p = 1, \ldots, M$. Then the right-hand side of Eq. (2) is formulated as follows:

$$|\tilde{\lambda}_m|^n \begin{bmatrix} A_{m,1} \exp\{\mathrm{i}(\omega_m n \Delta t - \boldsymbol{r}_1^{\mathsf{T}} \boldsymbol{k}_m)\} \\ \vdots \\ A_{m,M} \exp\{\mathrm{i}(\omega_m n \Delta t - \boldsymbol{r}_M^{\mathsf{T}} \boldsymbol{k}_m)\} \end{bmatrix}. \tag{3}$$

This shows that the oscillatory pattern of m-th KM describes a spatio-temporal wave propagating with the angular frequency ω_m and wavenumber vector $\boldsymbol{k}_m$.

3.2. Results

This subsection applies KMD to the data shown in Fig. 3. Here, we set $M = 24$ and $N = 55$ (corresponding to 9 hours). In this paper, we decompose KM $\tilde{\boldsymbol{V}}_m$ into the two components $\boldsymbol{V}_m^{\mathrm{A}} \in \mathbb{C}^{12}$ and $\boldsymbol{V}_m^{\mathrm{H}} \in \mathbb{C}^{12}$, where $\boldsymbol{V}_m^{\mathrm{A}}$ stands for the component on the atrium temperature and $\boldsymbol{V}_m^{\mathrm{H}}$ for the outlet temperature.

Table 1 shows the modal information on the data in decreasing order of the modulus $|\tilde{\lambda}_m|$. The eigenperiod is defined as:

$$T_m = \frac{2\pi \Delta t}{|\mathrm{Im}[\ln \tilde{\lambda}_m]|}. \tag{4}$$

The sampling period Δt is 10 min. Mode pair $\{m, m+1\}$ that has large values of $|\lambda_m|$ and $\|\tilde{\boldsymbol{V}}_m\|$ is dominant in the data. In this paper, we adopt mode pair $\{5, 6\}$ as the dominant one and utilize it to identify the heat transfer in the atrium.

Next, Fig. 4 shows the amplitude and phase of KMs $\boldsymbol{V}_5^{\mathrm{A}}$ and $\boldsymbol{V}_5^{\mathrm{H}}$. The arrows represent the directions of the wavenumbers $\boldsymbol{k}_5^{\mathrm{A}}$ of $\boldsymbol{V}_5^{\mathrm{A}}$ and $\boldsymbol{k}_5^{\mathrm{H}}$ of $\boldsymbol{V}_5^{\mathrm{H}}$. Note that $\boldsymbol{k}_5^{\mathrm{A}}$ and $\boldsymbol{k}_5^{\mathrm{H}}$

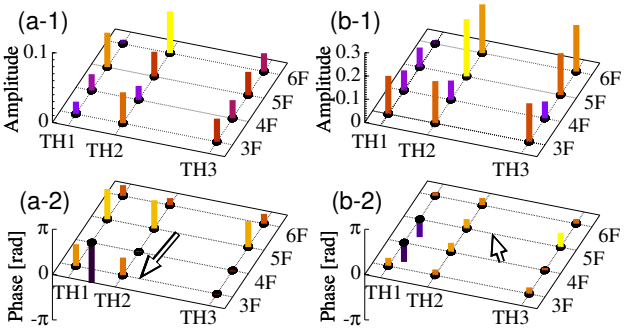

Figure 4: Amplitude and phase of KM $\tilde{\boldsymbol{V}}_5$ shown in Tab. 1: (a-1,a-2) $\boldsymbol{V}_5^{\mathrm{A}}$ of atrium temperature, where the arrow represents the direction of caluculated wavenumber vector $\boldsymbol{k}_5^{\mathrm{A}}$, and (b-1,b-2) $\boldsymbol{V}_5^{\mathrm{H}}$ of outlet temperature, where the arrow represents the direction of caluculated wavenumber vector $\boldsymbol{k}_5^{\mathrm{H}}$.

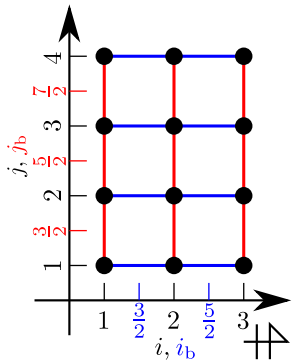

Figure 5: Nodes and brabches for space-discretization. The integer index i stands for the length x and j for the height z. The fractional indices i_{b} and j_{b} stand for the branch between nodes $[i, j]$.

are the two-dimentional vectors ($N_{\mathrm{d}} = 2$) calculated by replacing $\tilde{\boldsymbol{V}}_m$ with $\boldsymbol{V}_5^{\mathrm{A}}$ and $\boldsymbol{V}_5^{\mathrm{H}}$ in Eqs. (2) and (3). In Fig. 4(a-1,b-1), the amplitude changes in space, implying that the heat input from HVAC units propagates in the atrium. In Fig. 4(a-2,b-2), the phase also changes in space, and the wavenumber vector $\boldsymbol{k}_5^{\mathrm{H}}$ is in the opposite direction of $\boldsymbol{k}_5^{\mathrm{A}}$. This indicates that the HVAC units operate to decline the heat transfer in the atrium.

4. Identification of heat transfer in atrium

This section formulates the heat transfer in the target atirum as isotropic difusion equation, namely, *effective diffusion*. Then, the effective diffusion coefficient of the equation is identified with the KM $\tilde{\boldsymbol{V}}_5$ shown in Fig. 4.

4.1. Effective diffusion by small-scale air movement

The target atrium is regarded as the two-dimentional domain because the width of the atrium is much smaller than the length x and height z (see Figs. 1 and 2). Here, we introduce the concept of effective diffusion for describing the heat transfer in the two-dimentional domain. It is widely known that the homogenization makes it possible to represent the heat transfer caused by small-scale air movement as isotropic diffusion [5, 6]. In the target atrium, no large-scale laminar flow by HVAC outlets occurs, and hence the air moves on the scale less than the length between rooms. Therefore, by coarse-graining of the thermal dynamics on the length-scale larger than the distance between rooms, we represent the temperature T at position $\boldsymbol{x} := (x, z)^{\mathsf{T}} \in A \subset \mathbb{R}^2$ and time $t \in \mathbb{R}$ via the following diffusion equation:

$$\frac{\partial}{\partial t} T(\boldsymbol{x}, t) = D_{\mathrm{e}}(\boldsymbol{x}) \Delta T(\boldsymbol{x}, t) + \frac{P_{\mathrm{HVAC}}(\boldsymbol{x}, t) + e(\boldsymbol{x}, t)}{\rho c_{\mathrm{p}}}, \qquad (5)$$

where A is a closed domain of the atrium, D_{e} is the effective diffusion coefficient, P_{HVAC} is the heat input per unit time and unit volume from HVAC, e is the input from the other sources, ρ and c_{p} are the air density and the specific heat at constant pressure. P_{HVAC} is formulated as a function of outlet temperature T_{HVAC} (see Sec. 4.2)

4.2. Method for identifying D_{e}

This subsection provides the method for identifying D_{e}.

The diffusion equation model (5) is discretized with the integer indices $i \in \{1, 2, 3\}$ corresponding to TH1, TH2, and TH3, $j \in \{1, \ldots, 4\}$ to 3F–6F, and $n = 0, \ldots, N-1$ to the time-instant. Figure 5 shows the Staggered lattice [7] for discretization of the atrium. In this paper, the branches are denoted by $[i_{\mathrm{b}}, j]$ and $[i, j_{\mathrm{b}}]$ with the fractional indices $i_{\mathrm{b}} \in \{3/2, 5/2\}$ and $j_{\mathrm{b}} \in \{3/2, 5/2, 7/2\}$, and the effective coefficient D_{e} is defined on the branches. Note that the coefficient on $[i_{\mathrm{b}}, j]$ is influenced by the heat input $e(\boldsymbol{x}, t)$ due to the in-room thermal dynamics.

Next, we describe Eq. (5) based on KMD. Let us represent the component of KM $\boldsymbol{V}_m^{\mathrm{A}}$ on position $[i, j]$ with $v_m[i, j]$ and that of $\boldsymbol{V}_m^{\mathrm{H}}$ as $u_m[i, j]$. It is shown in [3] that each oscillatory pattern $\tilde{\lambda}^n \tilde{\boldsymbol{V}}_m$ is determined by its initial condition and does not interact with any others. Thus, we assume that the oscillatory pattern is a solution of the discretized equation of (5). In addition, it is now possible to neglect the contribution of $e(\boldsymbol{x}, t)$ in Eq. (5) because $e(\boldsymbol{x}, t)$—determined by the outdoor temperature and solar radiation—varies on the day scale and does not contribute to the hour-scale thermal dynamics. Thus, by substituting $\tilde{\lambda}_m^n v_m$ (or $\tilde{\lambda}_m^n u_m$) to T (or T_{HVAC}) in the discretized version of (5), the linear equation of $v_m[i, j]$ and $u_m[i, j]$ is derived as follows:

$$\begin{aligned} s_m v_m[i, j] = & \sum_{i_{\mathrm{b}} = i \pm \frac{1}{2}} D_{i_{\mathrm{b}}, j} \frac{v_m[i \pm 1, j] - v_m[i, j]}{L_{i_{\mathrm{b}}}^2} \\ & + \sum_{j_{\mathrm{b}} = j \pm \frac{1}{2}} D_{i, j_{\mathrm{b}}} \frac{v_m[i, j \pm 1] - v_m[i, j]}{H^2} \\ & + \frac{U_{\mathrm{HVAC}}}{V_0[i, j]} (u_m[i, j] - v_m[i, j]), \end{aligned} \qquad (6)$$

where the two $\pm$ signs of the first or second term of the right-hand side are in the same order, $s_m := \ln[\lambda_m]/\Delta t$ is the m-th eigen-angular frequency, and D with subscript of $i, i_{\mathrm{b}}, j, j_{\mathrm{b}}$ is the effective coefficient. The parameter $L_{i_{\mathrm{b}}}$ is

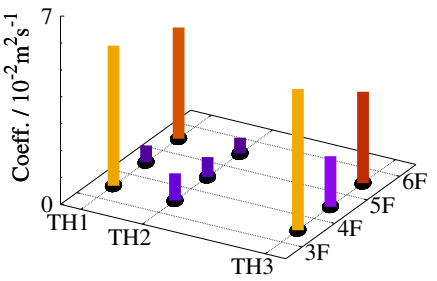

Figure 6: Caluculated effective coefficient D_e at branch $[i, j_b]$.

the discretization step at the branches $[i_b, j]$ and independent on j because the temperature sensors are at the same locations on every floor. The constant $H = 4.0\,\mathrm{m}$ is the length between rooms, $U_{\mathrm{HVAC}} = 0.875\,\mathrm{m}^3/\mathrm{s}$ is outlet volume rate of HVAC units, and $V_0[i, j]$ is the discretized volume of the node $[i, j]$ determined as shown in Figs. 1 and 2. The third term in the right-hand side of Eq. (6) is derived from the so-called bulk convection [1]. Moreover, we set a constraint condition for obtaining a physically-tractable solution of Eq. (6). Assuming that the air flow field is homogeneous because of no HVAC unit in the atrium, we introduce the following condition:

$$D_{i,j_b} = \frac{\dfrac{D_{i+1,j_b}}{L^2_{i+1/2}} + \dfrac{D_{i-1,j_b}}{L^2_{i-1/2}} + \dfrac{D_{i,j_b+1} + D_{i,j_b-1}}{H^2}}{\dfrac{1}{L^2_{i+1/2}} + \dfrac{1}{L^2_{i-1/2}} + \dfrac{2}{H^2}}. \tag{7}$$

Eq. (7) minimizes the discritized form of $\|\nabla D_e\|$ at the branch $[i, j_b]$, namely, the coefficient D_e does not drastically change in space. As a result, it is enough to solve Eqs. (6) and (7) for identifying the coefficient D_e.

4.3. Result

Here, we calculate D_e by the method in Sec. 4.2 and verify the result with the characteristic numbers of fluid flow in the atrium and its architectural geometry. The dominant KM $\tilde{V}_5$ was used for the calculation. Since the eigenperiod $T_5 = 3.35\,\mathrm{h}$ was small, it was reasonable in Eq. (6) to neglect the long-term dynamics. Also, we adopted the constraint condition (7) at the five nodes $[1, 5/2]$, $[2, 3/2]$, $[2, 5/2]$, $[2, 7/2]$, and $[3, 5/2]$ where the boundary conditions contributed less to the calculation than the other four nodes. Note that the coefficient matrix of linear equations (6) and (7) was not of full rank, and we hence used the corresponding psuedo-inverse matrix to determine D_e.

Figure 6 shows the calculated coefficient D_e at the branch $[i, j_b]$. Note that the coefficient at $[i_b, j]$ reflects the in-room thermal dynamics and does not quantify the effective diffusion in the atrium. The calculated coefficient is in the order of $10^{-2}\,\mathrm{m}^2/\mathrm{s}$, which value is tractable because of the following reason. Now we set the target length-scale L of the heat transfer at $H = 4.0\,\mathrm{m}$, the in-room air velocity U at $0.8\,\mathrm{m/s}$ based on the outlet volume of HVAC units, and the molecular diffusion coefficient D at $2.25\times10^{-5}\,\mathrm{m}^2/\mathrm{s}$ [8]. Then the nominal value of the effective coefficient is given as $\sqrt{DLU} = 8.5\times10^{-3}\,\mathrm{m}^2/\mathrm{s}$ [5, 6] and close to the order of the calculated coefficient. This suggests that the effective heat diffusion by small-scale air movement is dominant in the target atrium.

Next, the space-dependency of the coefficient is discussed. The coefficient takes the large values at $[i, j_b] = [1, 3/2], [1, 7/2], [3, 5/2], [3, 7/2]$. This is partly because of the architectural geometry of the building. On the 3rd floor, a booth covers the center ($[i, j_b] = [1, 3/2]$) of the atrium. Also, another office room is located on the 6th floor of the office room. Because these booth and room work as obstacle objects to the air flow, the coefficient is calculated as the large values at the nodes next to the objects.

5. Conclusion

This paper proposed a method for modeling of heat transfer dynamics in a building atrium via Koopman mode decomposition (KMD). First of all, KMD was applied to measured data on atrium temperature and outlet temperature of HVAC. Next, the heat transfer was modeled as a two-dimentional diffusion equation with an effective diffusion coefficient. Then, we proposed a method for identifying the coefficient by incorporating the spatio-temporal oscillatory pattern into the model. The coefficient calculated by the method shows that the small-scale air movement is dominant of the heat transfer in the atrium. Moreover, the space-dependency of diffusion is closely related to the architectural geometry of the atrium. Thus, the KMD-based method enables us to investigate the heat transfer driven by in-building HVAC systems.

References

[1] J.L.M. Hensen and R. Lamberts, eds., Building Performance Simulation for Design and Operation, Spon Press, 2011.

[2] G.J. Levermore, Building Energy Management Systems: Applications to Low-energy HVAC and Natural Ventilation Control, 2nd Edition, E & FN Spon, 2000.

[3] I. Mezić, "Spectral Properties of Dynamical Systems, Model Reduction and Decompositions," Nonlinear Dyn., vol.41, no.1, pp.309–325, 2005.

[4] C.W. Rowley, I. Mezić, S. Bagheri, P. Schlatter, and D.S. Henningson, "Spectral Analysis of Nonlinear Flows," J. Fluid Mech., vol.641, pp.115–127, 2009.

[5] M. Avellaneda and A.J. Majda, "An Integral Representation and Bounds on the Effective Diffusivity in Passive Advection by Laminar and Turbulent Flows," Commun. Math. Phys., vol.138, no.2, pp.339–391, 1991.

[6] A. Fannjiang and G. Papanicolaou, "Convection Enhanced Diffusion for Periodic Flows," SIAM J. Appl. Math., vol.54, no.2, pp.333–408, 1994.

[7] C.W. Hirt and B.D. Nichols, "Volume of Fluid (VOF) Method for the Dynamics of Free Boundaries," J. Comput. Phys., vol.39, no.1, pp.201–225, 1981.

[8] F. Kreith, Fluid Mechanics, CRC Press, 2000.